Available online at www.sciencedirect.com
ScienceDirect
Journal of Photochemistry and Photobiology A: Chemistry 186 (2007) 14–23
Journal of Photochemistry and Photobiology A:Chemistry
www.elsevier.com/locate/jphotochem

New photochemically stable riboflavin analogue—3-Methyl-riboflavin tetraacetate

Małgorzata Insińska-Rak [a], Ewa Sikorska [b], Jose L. Bourdelande [c], Igor V. Khmelinskii [d], Wiesław Prukała [a], Krzysztof Dobek [e], Jerzy Karolczak [e,f], Isabel F. Machado [g], Luis F.V. Ferreira [g], Ewa Dulewicz [a], Anna Komasa [a], David R. Worrall [h], Maciej Kubicki [a], Marek Sikorski [a,*]

[a] *Faculty of Chemistry, A. Mickiewicz University, Grunwaldzka 6, 60-780 Poznań, Poland*
[b] *Faculty of Commodity Science, Poznań University of Economics, al. Niepodległości 10, 60-967 Poznań, Poland*
[c] *Unitat de Química Orgànica, Universitat Autònoma de Barcelona, Bellaterra, Barcelona 08193, Spain*
[d] *Universidade do Algarve, DQB, FCT, Campus de Gambelas, 8005-117 Faro, Portugal*
[e] *Faculty of Physics, A. Mickiewicz University, Umultowska 85, 61-614 Poznań, Poland*
[f] *Centre of Ultrafast Laser Spectroscopy, A. Mickiewicz University, Umultowska 85, 61-614 Poznań, Poland*
[g] *Centro de Química-Física Molecular, Complexo Interdisciplinar, Instituto Superior Técnico, 1049-001 Lisbon, Portugal*
[h] *Department of Chemistry, Loughborough University, Leicestershire LE11 3TU, UK*

Received 18 May 2006; received in revised form 3 July 2006; accepted 6 July 2006
Available online 13 July 2006

Abstract

Spectroscopic and photophysical properties of a flavin analogue – 3-methyl-riboflavin tetraacetate – were studied in methanol, ethanol, water and acetonitrile. We compared experimental spectroscopic data with the results of theoretical predictions, obtained using the TD-DFT method. Based on these calculations, we assigned (π,π^*) symmetry to both the lowest excited singlet and triplet states. We found the title compound to be a very efficient photosensitizer of singlet oxygen production ($\phi_\Delta = 0.61$). The triplet state quantum yield of 3-methyl-riboflavin tetraacetate was determined as 0.54 in methanolic solutions. Photodegradation quantum yield measurements demonstrate that the title compound may be used as a much more stable substitute of riboflavin, being two orders of magnitude more photostable ($\varphi_R = 2 \times 10^{-5}$). We also present exhaustive crystallographic characteristics of 3-methyl-riboflavin tetraacetate, along with time-resolved fluorescence spectra of its polycrystals.

Keywords: Flavin analogue; 3-Methyl-riboflavin tetraacetate; Riboflavin; TD-DFT method; Triplet states; Photosensitizer; Singlet oxygen; Photodegradation; Crystallographic characteristics; Time-resolved fluorescence spectra

1. Introduction

Spectroscopy and photophysics of flavin-related compounds deserve much attention from a variety of points of view. Their redox reactivity is a crucial factor, which determines whether they participate in many natural processes. This parameter is the one most drastically changed by photoexcitation as compared to the ground state. For that reason, flavoenzymes and flavin analogues have been the subject of intense research for application as photocatalysts for biological redox processes [1]. Riboflavin is an important biological redox cofactor, essential to human and animal health [2]. Such strong reducing agents as nicotinamide nucleotides can transfer electrons to flavins in a thermodynamically allowed process. This process is catalysed by enzymes, which bind both cofactors to allow a very efficient intramolecular electron transfer [3]. Riboflavin is known to undergo photoreactions with nucleic acids and to sensitize the destruction of tumour cells and intra- and extra-cellular HIV particles [4,5].

Riboflavin can be used as a photodegradation sensitizer of many compounds in aqueous solutions. However, Larson et al. [6] report that its used as a photosensitizer is limited, due to its rapid photodecomposition. According to the author, the ribose chain of riboflavin facilitates its photodegradation and

* Corresponding author. Tel.: +48 61 8291309; fax: +48 61 8658008.
E-mail address: sikorski@amu.edu.pl (M. Sikorski).

1010-6030/$ – see front matter © 2006 Elsevier B.V. All rights reserved.
doi:10.1016/j.jphotochem.2006.07.005

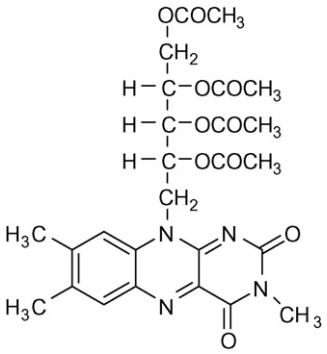

Fig. 1. Molecular structure of 3-methyl-riboflavin tetraacetate, 3MTARF.

also influences the yield and lifetime of its triplet excited state [6]. For recent reports on riboflavin photochemistry in water see for example [7–9].

The interesting photophysical properties of riboflavin encouraged us to study its tetraacetyl derivative. Moreover, the 2′,3′,4′,5′-tetraacetylated derivative revealed advantageous physicochemical properties, such as higher lipophilicity, which increases its ability to penetrate biological membranes [10].

In the above context we wish to discuss the spectroscopic and photophysical properties of 3-methyl-riboflavin tetraacetate, 3MTARF, which is a riboflavin analogue bearing a methyl group in position 3 of the isoalloxazine ring and hydroxyl groups in the side chain protected by acetyl substituents (see Fig. 1). In principle, this compound should have higher lipophilicity, which increases permeability through biological membranes. We also expected 3MTARF to be much more resistant to photodegradation compared to riboflavin and many of its derivatives that degrade photochemically very easily, which limits their possible applications.

To improve understanding of the properties of the title compound, we report steady-state spectra, time-dependent fluorescence emission spectra, theoretical predictions concerning singlet and triplet excited states (obtained using TD-DFT method), time-resolved luminescence emission spectra of polycrystals, and crystallographic data describing single molecules and molecular organization within the crystal structure due to intermolecular hydrogen bonds. We also confirm that this compound is a good singlet oxygen photosensitizer, which we believe to be one of the most interesting of its properties, and evaluate its improved photostability compared to riboflavin. The molecular structure of 3-methyl-riboflavin tetraacetate is presented in Fig. 1.

2. Experimental

2.1. Spectral, photophysical and photodegradation measurements

3-Methyl-riboflavin tetraacetate was a gift from Prof. A. Koziołowa. In order to obtain NMR spectra a Varian Gemini 300 MHz instrument was used. ^{1}H NMR (CD_3OD) δ: 7.87 (s, 1H, C_9–H), 7.79 (s, 1H, C_6–H), 3.41 (s, 3H, C_{31}–H), 2.48 (s, 3H, C_{71}–H), 2.63 (s, 3H, C_{81}–H), 5.68–4.20 (ribityl group, 5H, C_{11}–H, C_{14}–H), 2.25–1.69 (ribityl group, 12H, C_{123}–H, C_{133}–H, C_{143}–H, C_{153}–H).

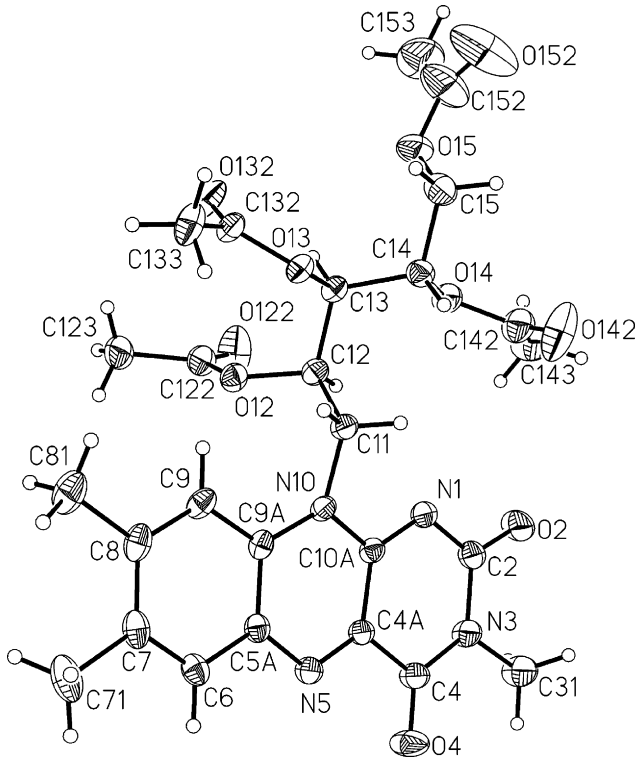

Fig. 2. Anisotropic-ellipsoid representation of 3-methyl-riboflavin tetraacetate together with the numbering scheme (hydrogen atoms were numbered according to their carrier atoms, *e.g.* those bonded to C71 are H71A, H71B and H71C, with their captions omitted for clarity). The ellipsoids are drawn at 50% probability level, hydrogen atoms are represented by spheres of arbitrary radii.

^{13}C NMR (CD_3OD) δ: 170.11, 169.58, 169.26 ((C_{122}), (C_{132}), (C_{142}), (C_{152})), 161.86 (C_4), 157.59 (C_2), 150.68 (C_{10a}), 149.31 (C_8), 138.48 (C_7), 136.69 (C_{4a}), 135.96 (C_{5a}), 132.93 (C_{9a}), 132.69 (C_6), 117.57 (C_9), 71.67 (C_{13}), 70.76 (C_{12}), 70.63 (C_{14}), 62.99 (C_{15}), 45.71 (C_{11}), 28.87 (C_{31}), 21.34 (C_{81}), 20.99 (C_{71}), 20.70, 20.56, 20.30, 19.30 ((C_{123}), (C_{133}), (C_{143}), (C_{153})), with the atom numbering shown in Fig. 2; see also NMR data in Ref. [11,12]. The FTIR spectra were measured on a Bruker IFS 66v/S instrument, which was evacuated to avoid water and CO_2 absorptions. Each spectrum included 64 scans at 31 °C. The spectra were measured in Nujol and Fluorolube mulls and are presented in Fig. 1 of the Supporting Information to this paper. All solvents were of spectroscopic or HPLC grade (Aldrich, Merck) and were used as received with the exception of acetonitrile, which was dried by refluxing over calcium hydride immediately before use. The purity of the solvents was additionally confirmed by the absence of fluorescence at the maximum sensitivity of the spectrofluorometer.

All experiments were carried out at room temperature. UV–vis absorption spectra were recorded on a Varian Cary 5E spectrophotometer. Steady-state fluorescence spectra were recorded on a Jobin Yvon-Spex Fluorolog 3–11 spectrofluorometer. Fluorescence quantum yields were determined using quinine sulphate in 0.1 M H_2SO_4 as a standard ($\phi_F = 0.52$) [13]. Fluorescence lifetimes were measured using excitation at

380 nm and the single photon timing technique on a fluorescence lifetime spectrophotometer, which has been described in detail elsewhere [14].

Transient absorption measurements were performed by using the nanosecond laser flash photolysis system available in Barcelona, with right-angle geometry. The LKS60 instrument from Applied Photophysics was used employing the third harmonic (355 nm) of a Q-switched Nd:YAG laser (Spectron laser system, UK; pulse width *ca.* 9 ns) for laser flash excitation.

Singlet oxygen luminescence experiments were performed by excitation of the sample with the third harmonic (355 nm) of a Nd:YAG laser (Lumonics hyperYAG HY200, 2 mJ/pulse, 8 ns FWHM). The excitation energy was attenuated by solutions of sodium nitrite in water. Detection was obtained on an EO-980P liquid nitrogen cooled germanium photodiode detector (*North Coast Scientific*), with a 1270 nm interference filter (*Melles Griot*) interposed between sample and detector in order to reduce detection of laser scatter and sensitizer emission, and to isolate the singlet oxygen phosphorescence. Data were captured with a 250MS/s digitizing oscilloscope (*Tektronix* 2432A) and Microcal Origin was used in data analysis. Perinaphthenone (Aldrich) was used as a reference standard for the singlet oxygen yield, $\phi_\Delta = 0.95 \pm 0.05$, independent on solvent [15].

Triplet state quantum yields were determined using the method of Wilkinson et al. [16,17]. Briefly, bromobenzene was used as a heavy-atom quencher, and both the reduction in fluorescence and the concomitant increase in triplet–triplet absorption were measured as a function of quencher concentration in deoxygenated solution. The triplet state quantum yield is then the slope of a plot of F_0/F versus $((F_0/F) \times (T/T_0) - 1)$, with F and T the intensities of fluorescence and triplet–triplet absorption, respectively. Fluorescence intensities were measured using a Spex 3-FluoroMAX spectrofluorometer, and transient absorption measurements made using excitation with the third harmonic of a Continuum Surelite I Nd:YAG laser (5 ns pulse width). Detection of the 275 W Xenon source was with a Hamamatsu R928 photomultiplier tube, the output from which was digitised with a LeCroy Waverunner LT364 oscilloscope.

Laser Induced Fluorescence (LIF) emission measurements of powdered crystalline samples were performed at room temperature, in a front surface arrangement. A detailed description with a diagram of the system has been presented in reference [18]. The system used the 337.1 nm pulse of a N_2 laser (Photon Technology Instruments, Model 2000, *ca.* 600 ps FWHM, ~1.3 mJ/pulse) as the excitation source. The light arising from the irradiation of solid samples by the laser pulse was collected by a collimating beam probe coupled to an optical fibre (fused silica) and detected by a gated intensified charge coupled device (ICCD, Oriel model Instaspec V). The ICCD was coupled to a fixed imaging compact spectrograph (Oriel, model FICS 77441). The system can be used either by capturing all light emitted by the sample or in the time-resolved mode by using a delay generator (Stanford Research Systems, model DG535) and a suitable gate width. The ICCD has high speed (2.2 ns) gating electronics and covers the 200–900 nm wavelength range [18–20].

Photodegradation of 3-methyl-riboflavin tetraacetate was studied using riboflavin for comparison. High-pressure mercury arc lamp, type HBO-200, was used as the radiation source. The radiation around $\lambda = 365$ nm was selected using a suitable interference filter and a Wood's filter. Methanolic solution of the two compounds at *ca.* 10^{-6} M were irradiated in a cylindrical quartz cell ($V = 2.8$ ml, $l = 1$ cm). After an appropriate exposure time, absorption spectra were recorded in the 200–700 nm spectral range. Chemical actinometry with Reinecke salt was used to measure the energy absorbed by the samples. Solutions of Reinecke salt were irradiated in the same conditions, yielding 8.8×10^{15} photons absorbed by the actinometer in 60 s. Apparent quantum yields extrapolated to zero irradiation time gave real quantum yields of photodegradation (φ_R). The complete procedure was described in detail in [21].

2.2. TD-DFT calculations

The electronic structure and geometry of 3-methyl-riboflavin tetraacetate were obtained using density-functional theory (DFT) quantum-chemical calculations [22]. The calculations were performed using the B3LYP functional [23] in conjunction with a modest 6-31G-(d) split-valence polarized basis set [24]. Excitation energies and oscillator strengths in the dipole length representation were calculated for the optimized ground-state geometries using the time-dependent (TD) approach as implemented in the Gaussian 03 package of *ab initio* programmes [25]. The lowest-energy singlet-singlet transitions, $S_0 \rightarrow S_i$, were calculated for the ground-state geometry. The excitation energies computed at the B3LYP/6-31G(d) level of theory were estimated to be accurate within 2000–3000 cm^{-1}, usually requiring a shift to the red to reproduce experimental spectra. In the present work the $T_1 \rightarrow T_i$ excitation energies and transition intensities were determined for the optimized geometry of the lowest triplet state (T_1). We used the unrestricted UB3LYP approach in calculations of the $T_1 \rightarrow T_i$ spectra.

2.3. X-ray diffraction analysis

A crystal of 3-methyl-riboflavin tetraacetate was analysed at 100(1) K on an Oxford Diffraction KM4CCD diffractometer with graphite-monochromated Mo Kα radiation ($\lambda = 0.71073$ Å). The data were collected using the ω-scan technique to a maximum θ value of 30 °C and corrected for Lorenz and polarization effects. The structure was solved with SHELXS97 [26] and refined by the full-matrix least-squares method with SHELXS97 [27]. Non-hydrogen atoms were refined anisotropically, and hydrogen atoms were put in idealized positions and refined isotropically using the riding model with U_{iso} values set at 1.2 (1.4 for methyl groups) times U_{eq} of the appropriate carrier atom.

3. Results and discussion

Riboflavin and its derivatives had been the subject of intense studies, in order to explain their interesting properties and to study their possible applications. They owe their important role in living organisms and the variety of their applications to the isoalloxazine ring system, which enables them to mediate

Table 1
Crystal structure and structure refinement parameters of 3-methyl-riboflavin tetraacetate

Chemical formula	$C_{26}H_{30}N_4O_{10}$
Formula weight	558.54
Crystal system	Monoclinic
Space group	$P2_1$
a (Å)	12.989(1)
b (Å)	7.216(1)
c (Å)	15.511(1)
β (°)	90.067(8)
Volume, V (Å^3)	1453.8(3)
Z	2
Calculated density, D_x (g/cm^3)	1.28
μ	0.099
Reflections	
Collected	8740
Independent [R_{int}]	2753 [0.040]
$R[I > 2\sigma(I)]$	0.059
wR2 [all data]	0.156
Goodness of fit, S	1.16
Max/min $\Delta\rho$ (Å)	0.48/−0.30

Crystallographic data, tables of atomic coordinates, thermal parameters, bond lengths and bond angles have been deposited with the Cambridge Crystallographic Data Centre, CCDC, with the deposition No. CCDC 273717. Copies of this information may be obtained free of charge from the Director, CCDC, 12 Union Road, Cambridge CB2 1EZ, UK (fax: +44 1223 336 033; email: deposit@ccdc.cam.ac.uk or http://www.ccdc.cam.ac.uk).

Table 2
Torsion angles (°) that describe the conformation of the side chain

C10A–N10–C11–C12	89.1(4)
C9A–N10–C11–C12	−101.1(4)
N10–C11–C12–C13	176.0(3)
C11–C12–C13–C14	61.0(4)
C12–C13–C14–C15	178.0(4)
N10–C11–C12–O12	60.0(4)
C11–C12–C13–O13	−58.0(4)
C12–C13–C14–O14	57.4(4)
C13–C14–C15–O15	−64.9(4)

electron-transfer processes over a wide range of redox potentials [1]. Presently, we took an insight into the molecular structure, spectroscopy, photophysics and photochemistry of 3-methyl-riboflavin tetraacetate, showing that experimental results support the data obtained by theoretical calculations. Therefore, we were able to explain some of the properties of the title compound.

We investigated the structure of 3-methyl-riboflavin tetraacetate by X-ray diffraction, with the crystallographic data obtained summarized in Table 1. Fig. 2 shows the anisotropic-displacement-ellipsoid representation of the molecule obtained from treatment of the X-ray diffraction data. The bond lengths and angles agree well with those found in related compounds. The planarity of the three-ring system is reasonable; the dihedral angle between terminal benzene and uracil moieties is 3.40(4)°, and agrees well with the values found in *e.g.* riboflavin tetraacetate acetone solvate monohydrate (1.6(2)° and 2.4(2)° for two symmetry-independent molecules) [28]. The conformation of the side chain can be described by five torsion angles (Table 2). The value of the C10A–N10–C11–C12 torsion angle, of 89.1(4)°, shows that the molecule is in the so-called P-conformation; the conformation along the chain may be described as t–g$^+$–t.

The molecules in the crystal structure are organized into infinite stacks along the [0 1 0] direction (Fig. 3, the distance between the median planes of the riboflavin moieties is *ca.* 3.6 Å), and the molecules in the single stack are additionally connected by the relatively short C–H···O hydrogen bonds. The stacks are bound only weakly one to another, also by C–H···O interactions (Fig. 4). The geometrical details of these hydrogen bonds are listed in Table 3.

The investigated compound – 3-methyl-riboflavin tetraacetate – absorbs light in the UV–vis region. The absorption spec-

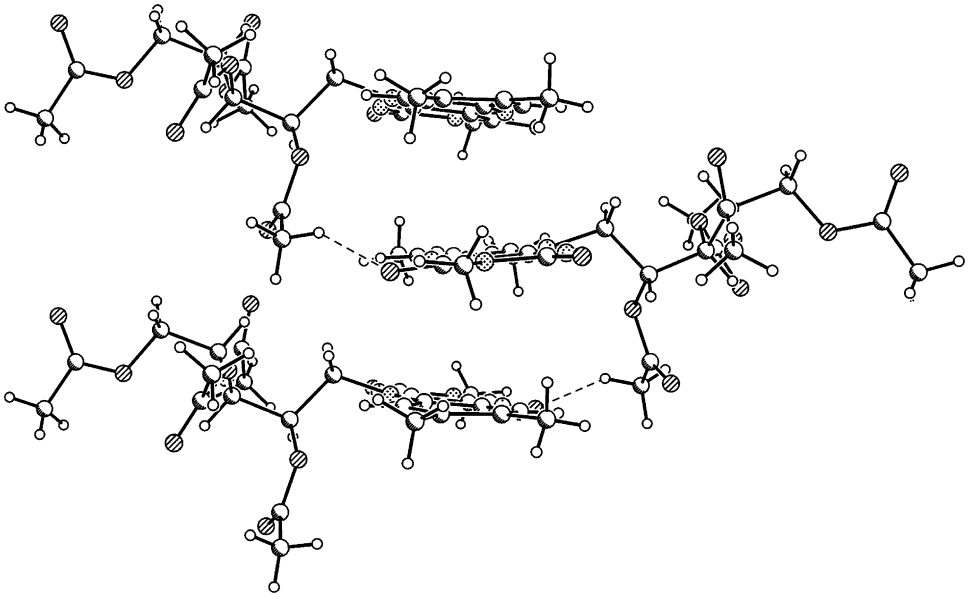

Fig. 3. A fragment of the stack of 3-methyl-riboflavin tetraacetate molecules as seen approximately along the [4 0 1] direction; C–H···O hydrogen bonds are shown as dashed lines.

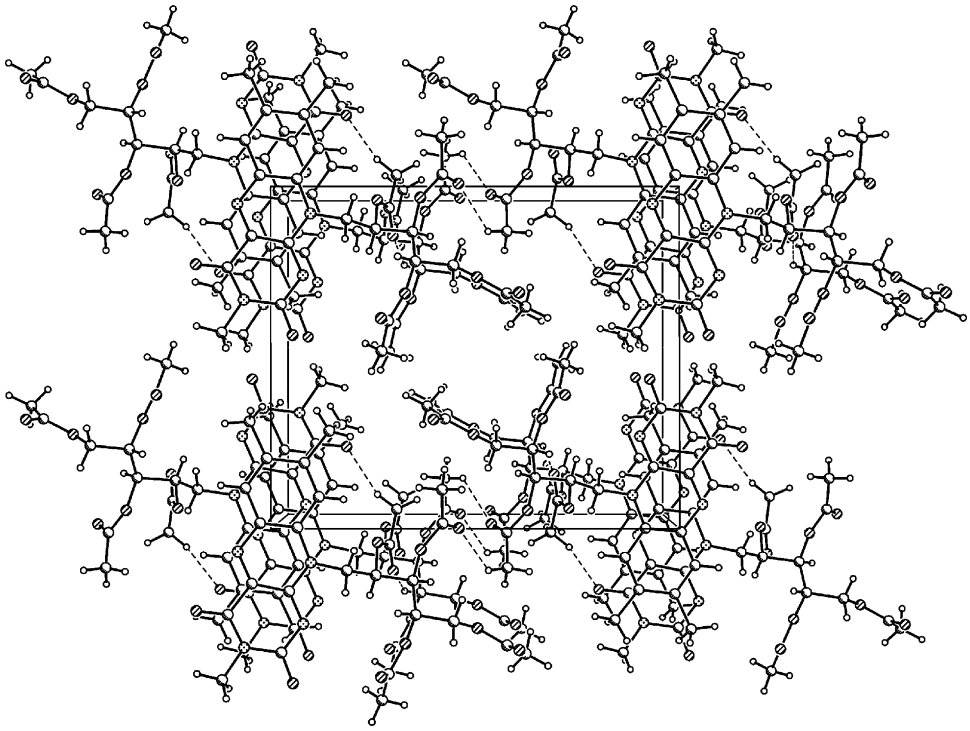

Fig. 4. Crystal packing of 3-methyl-riboflavin tetraacetate as seen along the [0 1 0] direction; C–H···O hydrogen bonds are shown as dashed lines.

Table 3
The C–H···O hydrogen bond data

D	H	A	D–H (Å)	H···A (Å)	D···A (Å)	D–H···A (°)
C123	H12D	O4^{i}	0.96	2.37	3.203(6)	145
C123	H12B	O13^{ii}	0.96	2.59	3.503(6)	158
C133	H13B	O132^{iii}	0.96	2.44	3.153(7)	132
C15	H15A	O132^{iii}	0.96	2.60	3.558(6)	171
C14	H14A	O122^{iv}	0.96	2.53	3.389(6)	147

D, H, and A are donor, hydrogen atom, and acceptor of a hydrogen bond, respectively. Symmetry codes: (i) $-x$, $-1/2+y$, $2-z$; (ii) x, $-1+y$, z; (iii) $-x$, $1/2+y$, $1-z$; (iv) x, $1+y$, z.

trum in methanol consists of several bands—227, 275, 353, and 448 nm (46.0, 36.4, 28.3, and 22.3×10^3 cm^{-1}, respectively). The positions of the absorption bands differ only slightly from those in riboflavin, due to the presence of the methyl substituent in position N(3) of the isoalloxazine ring and hydroxyl groups in the side chain protected by acetyl substituents. The compound fluoresces at room temperature ($\phi = 0.089$ in methanol). The fluorescence emission in methanol appears as a single structureless band with the maximum at 513 nm (19.5×10^3 cm^{-1}). The absorption and fluorescence excitation spectra remain in good agreement with each other. The fluorescence decay is described by a single-exponential function, as confirmed by statistical "goodness-of-fit" criteria, with fluorescence lifetime $\tau_F = 5.4$ ns. All these results are collected in Table 4, along with other spec-

Table 4
Spectroscopic and photophysical data for the first singlet excited state of 3-methyl-riboflavin tetraacetate and riboflavin in different solvents

Compound	Solvent	λ_2 (nm)	λ_1 (nm)	λ_F (nm)	ϕ_F	τ_F (ns)	k_r (10^8 s^{-1})	$\sum k_{nr}$ (10^8 s^{-1})
3MTARF	Acetonitrile	345	446	505	0.12	5.8	0.21	1.5
	Methanol	353	448	513	0.089	5.4	0.16	1.7
	Ethanol	351	449	512	0.064	5.5	0.12	1.7
	Water	373	451	520	0.11	4.4	0.25	2.0
Riboflavin	Water	375	447	537	0.28	5.1	0.55	1.4
	Methanol	360	444	532	0.39[a]	5.21, 6.3, 5.4[a,b]	0.62	0.97

λ_1, λ_2 are the positions of the two lowest-energy bands in the absorption spectra, λ_F the fluorescence emission maximum, ϕ_F the fluorescence quantum yield, τ_F the fluorescence lifetime, k_r the radiative rate constant and $\sum k_{nr}$ the sum of non-radiative rate constants. The estimated relative error of ϕ_F and τ_F is 10%.

[a] Data from Ref. [39].

[b] Data from Ref. [40].

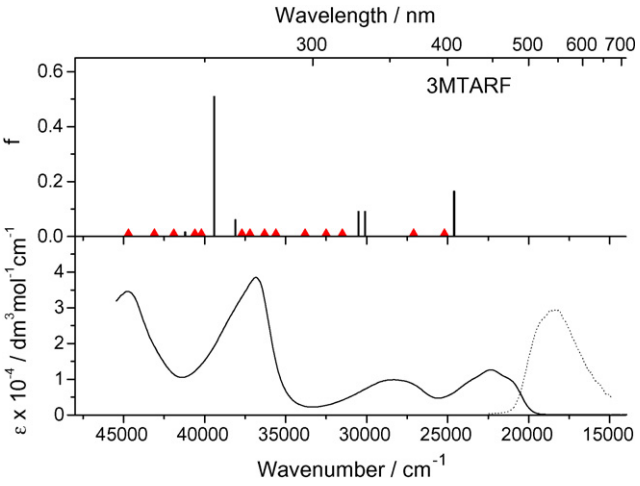

Fig. 5. Predicted lowest-energy singlet-singlet transitions of 3-methyl-riboflavin tetraacetate (top) compared to the experimental spectrum (bottom). Triangles mark the energies of the weak n,π* transitions, vertical bars show intensities and energies of the π,π* transitions. Fluorescence emission spectrum of 3MTARF in methanol is also shown as a dotted line. The experimental spectra were taken in methanolic solutions.

troscopic and photophysical parameters. The values of the rate constants for the radiative (k_r) and non-radiative ($\sum k_{nr}$) decay for the lowest excited singlet state were calculated as $k_r = \phi_F/\tau_F$ and $\sum k_{nr} = (1 - \phi_F)/\tau_F$, respectively. In all of the solvents examined, the decay of the singlet excited state is dominated by non-radiative phenomena. Interestingly, the highest radiative rate constants were obtained in acetonitrile and water, which is especially interesting if compared to ethanol where k_r is lower by a factor of *ca.* 2. These results are probably explained by specific solvent interactions and/or the *proximity effect* (see the following paragraph). Fig. 5 compares the experimental absorption spectrum of 3MTARF in methanol with the results of theoretical calculations for the lowest-energy singlet-singlet transitions, represented by bars proportional to the oscillator strengths of the respective transitions.

The electronic structure of 3-methyl-riboflavin tetraacetate was studied by means of time-dependent density-functional theory (TD-DFT) [22]. There are two intense absorption bands in the experimental data at about 353 and 448 nm (28.3 and $22.3 \times 10^3\,cm^{-1}$), which correspond to the two calculated lowest-energy π–π* transitions, located at 332 and 406 nm (30.1 and $24.6 \times 10^3\,cm^{-1}$). Close to the two observable π–π* transitions mentioned above, there exist two n–π* transitions of low oscillator strength located at 27.1 and $25.2 \times 10^3\,cm^{-1}$. The energy gap between π–π* and n–π* transitions is in the $(0.6–3.0) \times 10^3\,cm^{-1}$ range. This result is typical for isoalloxazines, which are known to have closely spaced low-lying π–π* and n–π* excited states. In the case of 3MTARF the energy gap between these states is only $600\,cm^{-1}$, very close to the same value in riboflavin, which is $900\,cm^{-1}$ [29]. As a consequence, some of the photophysical properties of the title compound may be understood on the basis of the proximity effect theory [30,31], which interprets the properties of such molecules as a result of vibronic interaction between the lowest π–π* and n–π* singlet states.

TD-DFT calculations predict the nature of molecular orbitals mainly involved in the predominant excitation. Based on these calculations, we conclude that the $S_0 \rightarrow S_1$ transition has a dominant contribution from the HOMO → LUMO excitation and can be interpreted as an allowed π–π* transition. Fig. 6 shows

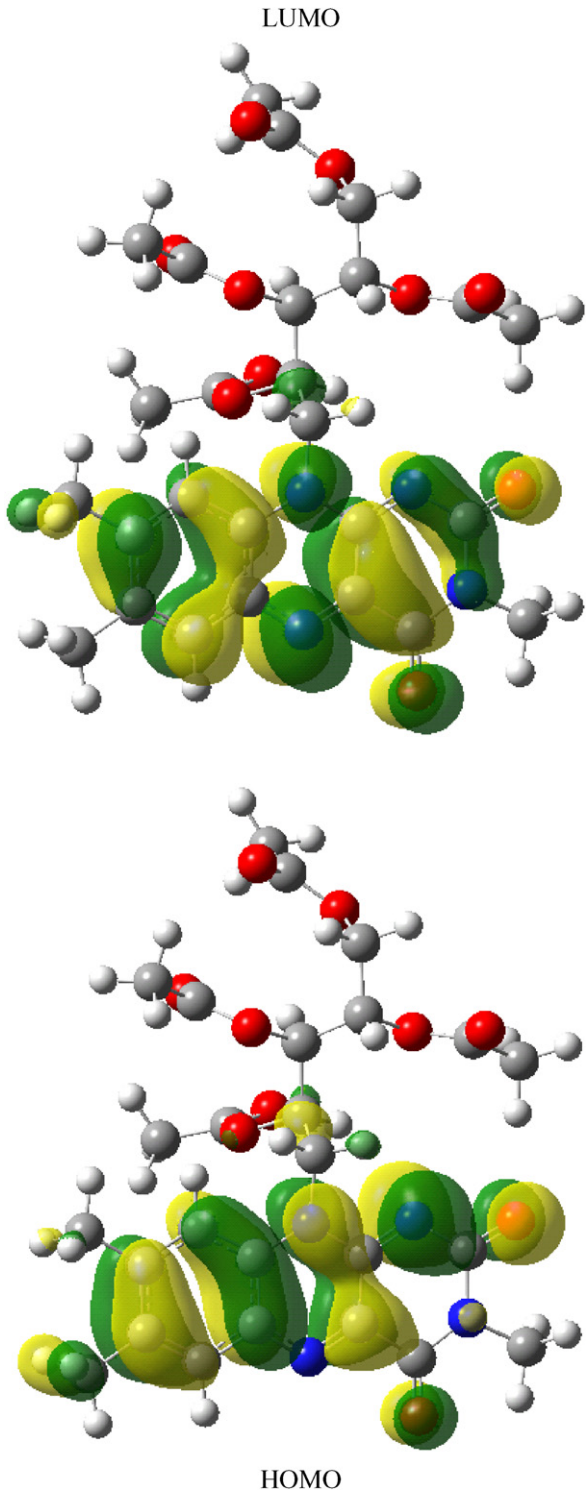

Fig. 6. The shape of the highest occupied (HOMO) and the lowest unoccupied (LUMO) molecular orbitals of 3-methyl-riboflavin tetraacetate, mainly involved in the lowest-energy transitions. The isosurfaces correspond to the value of ±0.02.

Table 5
Predicted (B3LYP/6–31G(d)) singlet ($S_0 \rightarrow S_i$) and triplet ($S_0 \rightarrow T_i$) excitation energies starting from the ground state and calculated (UB3LYP/6–31G(d)) triplet ($T_1 \rightarrow T_i$) excitation energies starting from the lowest triplet state of 3-methyl-riboflavin tetraacetate, with their corresponding oscillator strengths, f

$S_0 \rightarrow S_i$	E ($\times 10^{-3}$ cm^{-1})	f	$S_0 \rightarrow T_i$	E ($\times 10^{-3}$ cm^{-1})	f	$T_1 \rightarrow T_i$	E ($\times 10^{-3}$ cm^{-1})	f
$^1(\pi,\pi^*)$	24.6, **22.3**	0.165	$^3(\pi,\pi^*)$	16.9	0	$T_1 \rightarrow T_2$	7.4	0.006
$^1(n,\pi^*)$	25.2	0.002	$^3(n,\pi^*)$	22.3	0	$T_1 \rightarrow T_3$	7.7	0.001
$^1(n,\pi^*)$	27.1	0.002	$^3(\pi,\pi^*)$	22.5	0	$T_1 \rightarrow T_4$	8.6	<0.001
$^1(\pi,\pi^*)$	30.1, **28.3**	0.091	$^3(n,\pi^*)$	24.3	0	$T_1 \rightarrow T_5$	11.1	0.005
$^1(\pi,\pi^*)$	30.5	0.091	$^3(\pi,\pi^*)$	25.7	0	$T_1 \rightarrow T_6$	13.9	0
$^1(n,\pi^*)$	31.5	0				$T_1 \rightarrow T_7$	15.2	0.026
$^1(n,\pi^*)$	32.5	<0.001				$T_1 \rightarrow T_8$	16.2	0
$^1(n,\pi^*)$	33.8	0.002				$T_1 \rightarrow T_9$	17.3	<0.001
$^1(n,\pi^*)$	35.6	0				$T_1 \rightarrow T_{10}$	18.1	0.063
$^1(n,\pi^*)$	36.3	0.002				$T_1 \rightarrow T_{11}$	18.5	0.060
$^1(n,\pi^*)$	37.2	0.004						
$^1(n,\pi^*)$	37.7	0.007						
$^1(\pi,\pi^*)$	38.1	0.061						
$^1(\pi,\pi^*)$	39.4	0.510						
$^1(n,\pi^*)$	40.2	0.005						

The energy of the first triplet state calculated using the unrestricted formalism (UB3LYP/6-31G(d)) is 16.0×10^3 cm^{-1}. Experimental values taken in methanolic solutions are listed in bold type for comparison.

the shapes of the highest occupied (HOMO) and the lowest unoccupied (LUMO) molecular orbitals, mainly involved in the transitions to the low-lying excited states.

Based on the TD-DFT calculations, we can also predict the nature of the molecular orbitals involved in the $S_0 \rightarrow T_i$ excitations and the symmetry of the corresponding T_i excited states. Using the data presented in Table 5 we see that the $S_0 \rightarrow T_i$ excitation is a $^3(\pi,\pi^*)$ transition, with the dominant contribution from the HOMO → LUMO excitation.

The electronic structure of 3-methyl-riboflavin tetraacetate in its triplet state was described using experimental transient absorption spectrum in comparison with the results of theoretical calculations. Transition intensities and triplet–triplet excitation energy accompanied by their oscillator strengths were determined for the optimised geometry of the lowest triplet state (T_1), using the unrestricted UB3LYP/6-31G(d) formalism. The experimental transient absorption spectrum is presented in Fig. 7. The calculated values are available in Table 5 for comparison. The detectable transitions in 3-methyl-riboflavin tetraacetate are located at about 15,200, 18,100 and 18,500 cm^{-1}. Because of the considerable size of the molecule and its non-rigid structure, we were only able to calculate 10 lowest-energy $T_1 \rightarrow T_i$ transitions.

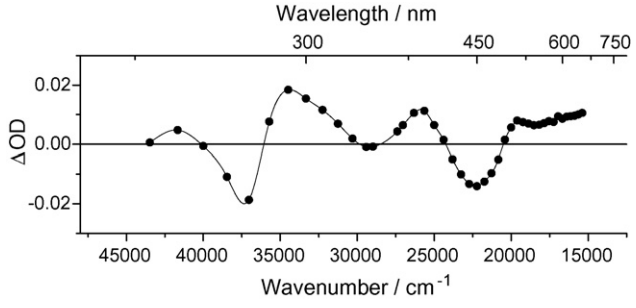

Fig. 7. The experimental transient absorption spectrum of 3-methyl-riboflavin tetraacetate in methanol excited at 355 nm, $OD_{355} = 0.297$, 2 mJ/pulse, $l = 1$ cm.

The above observations allowed us to study the interaction between 3-methyl-riboflavin tetraacetate and dissolved oxygen under irradiation. The measurements of singlet oxygen quantum yields with flavins as photosensitizers meet with several difficulties, thus there is a lack of data concerning this subject [32,33]. The method we used is based on measuring the emission at 1270 nm, which is highly specific to the $O_2(^1\Delta_g) \rightarrow O_2(^3\Sigma_g^-)$ transition, under laser excitation at 355 nm of methanolic solutions of the investigated compound. We examined air-equilibrated, oxygen-saturated, and N_2-purged sample solutions. With the increase of oxygen concentration we have observed a significant increase of emission intensity at the analytical wavelength (1270 nm). The values of quantum yield and lifetime of singlet oxygen formed by triplet photosensitisation were determined on the basis of data obtained for excited air-saturated solutions of the compound. Table 6 presents the data concerning the triplet state, triplet state lifetime, and the quantum yield and lifetime of singlet oxygen produced by 3-methyl-

Table 6
Triplet state lifetimes, τ_T, quantum yields of photosensitized production of singlet oxygen, ϕ_Δ, and singlet oxygen lifetimes, τ_Δ, for selected riboflavin derivatives in methanolic solutions

Compound	τ_T (μs)	ϕ_Δ	τ_Δ (μs)
Lumiflavin[a]	17	0.48	10
3-Methyl-lumiflavin[b]		0.53	10
3-Ethyl-lumiflavin[b]	9.5	0.55	10
3-Benzyl-lumiflavin[b]	34.9	0.53	10
Riboflavin[c]	3.7	0.51	10
Iso-(6,7)-riboflavin[c]	11	0.70	10
5-Deaza-riboflavin[d]	105	0.33	10
3MTARF[e]	20	0.61	10

[a] Data from Ref. [41].
[b] Data from Ref. [35].
[c] Data from Ref. [29].
[d] Data from Ref. [36].
[e] The triplet state quantum yield of 3-methyl-riboflavin tetraacetate was determined by us as 0.54 in methanolic solutions.

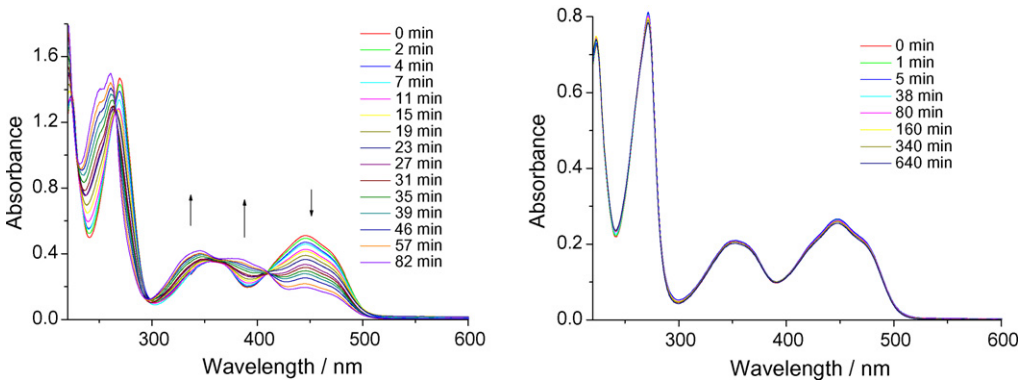

Fig. 8. UV and visible absorption spectra of photodegraded solutions of riboflavin (left panel) and 3-methyl-riboflavin tetraacetate (right panel) in methanol irradiated at 365 nm.

riboflavin tetraacetate photosensitisation. The relevant values for the flavin derivatives bearing various substituents in position N(3) of the lumiflavin ring and for those with ribityl chain in the structure are given for comparison. On the basis of these data we conclude that the value of the emission lifetime presently obtained ($\tau_\Delta = 10\ \mu s$) is typical for singlet oxygen in methanol [32,33]. The value of the singlet oxygen quantum yield is not affected by the presence of the ribityl chain, being slightly higher for the presently studied derivative with acetylated hydroxyl groups. The triplet state quantum yield was determined as 0.54 in methanolic solutions. Within the errors associated with measurements of the triplet state quantum yield and the quantum yield of singlet oxygen production of 0.61, both of which we estimate as 10%, these numbers may be regarded as approximately equal. Therefore, the efficiency of singlet oxygen production following triplet state quenching, f_Δ^T, is essentially unity. Thus, for this compound the quantum yield of singlet oxygen production gives a measure of the triplet state quantum yield. This high value of f_Δ^T suggests that triplet state quenching proceeds without any involvement of charge transfer interactions [34], probably as a result of charge-transfer states in these compounds being higher in energy than the corresponding triplet states. Further studies are underway to determine values of f_Δ^T for a series of similar compounds, to explore this observation further.

The photodegradation quantum yields are important both for possible applications, and in order to evaluate the feasibility of using the present compound as a model for riboflavin. These were examined in methanol for both 3-methyl-riboflavin tetraacetate and riboflavin. The results show that 3-methyl-riboflavin tetraacetate is at least two orders of magnitude more stable, the quantum yields obtained are 2×10^{-5} and 3×10^{-3}, for 3-methyl-riboflavin tetraacetate and riboflavin, respectively, both irradiated at 365 nm in air-equilibrated methanolic solutions. The stability of 3-methyl-riboflavin tetraacetate irradiated at 365 in methanol is clearly demonstrated in Fig. 8, where the UV and visible spectra of 3-methyl-riboflavin tetraacetate and riboflavin are shown for direct comparison (Fig. 9).

We also performed time-resolved fluorescence measurements of 3-methyl-riboflavin tetraacetate polycrystals, to study the effect of the crystal packing on the photophysical properties. The spectrum obtained upon excitation at 337 nm reveals an

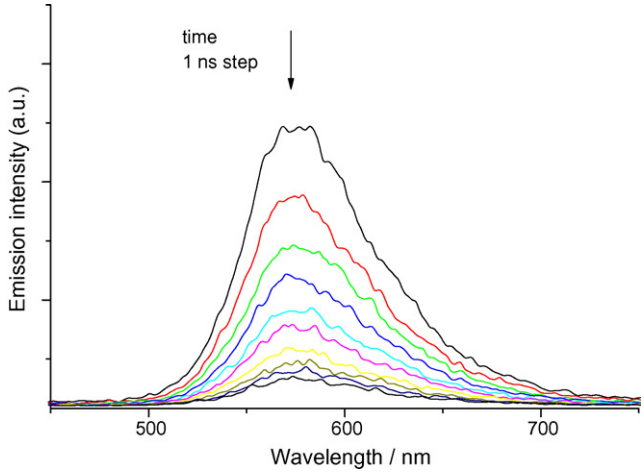

Fig. 9. Time-resolved fluorescence spectra of 3-methyl-riboflavin tetraacetate polycrystals, excitation at 337 nm. Spectra were recorded with 1 ns time step; the band maximum is at about 575 nm.

emission maximum at 575 nm ($17.4 \times 10^3\ cm^{-1}$), which is very different from the value obtained in methanolic solutions (see Table 4). Thus, the fluorescence emission of polycrystals originates from molecules interacting via hydrogen bonds, in agreement to what is observed in other lumichrome derivatives [29,35–37]. Note that riboflavin photodegrades very rapidly in riboflavin microparticles [38], similarly fast photodecomposition of polycrystalline *iso*-(6,7)-riboflavin has been noted recently by us [29]. In these compounds, a new fluorescence band with a maximum at about 420 nm appears upon irradiation in addition to the well-known riboflavin fluorescence band. The new emission has been attributed to alloxazine formed by photodegradation of riboflavin [38]. In comparison, polycrystalline 3-methyl-riboflavin tetraactetate is very stable, without any new fluorescence noticeable even after prolonged irradiation, indicating that this derivative is much more light-resistant and opening interesting possibilities for its future applications.

4. Conclusions

The work presented describes spectroscopic and photophysical properties of 3-methyl-riboflavin tetraacetate. In order to

interpret the results of experimental measurements, we applied time-resolved density functional theory to calculate excitation energies and symmetry of the excited states. The results obtained in this work lead us to a conclusion that the lowest excited singlet and triplet states of the molecule are of the π–π^* character. The lowest excited singlet state (π–π^*) has a closely neighbouring n–π^* state. Some authors suggest that there could be some sort of intramolecular hydrogen bonding of the ribityl hydroxyl group to the ring nitrogen under some conditions, though no evidence of such bonding is seen in the X-ray crystal structure of riboflavin [4,5]. If these suggestions were correct, acetyl substituents, present in the ribityl chain, would prevent formation of some of these hypothetical hydrogen bonds and thus influence the properties of 3MTARF, contrary to the recently obtained results. On the other hand, the X-ray results demonstrate the existence of several relatively short intermolecular C–H···O hydrogen bonds, which determine the crystal packing. The three-ring system is almost planar, which is typical in such compounds.

The compound investigated is good photosensitizer of singlet oxygen when excited in aerated environments, similar to other riboflavin analogues. It is also two orders of magnitude more photostable than riboflavin, with the phototodegradation quantum yield of $\varphi_R = 2 \times 10^{-5}$, which allows to use it as a model for the latter.

Acknowledgments

We thank Dr. Siân L. Williams (Loughborough) for her help in singlet oxygen experiments. Interdisciplinary grant No. 51103-504 from A. Mickiewicz University and University of Economics, Poznań, Poland, to MS and ES is gratefully acknowledged. The fluorescence lifetime measurements were performed at the Centre for Ultrafast Laser Spectroscopy, Adam Mickiewicz University, Poznań, Poland. The calculations were performed at the Poznań Supercomputing and Networking Centre (PCSS).

Appendix A. Supplementary data

Supplementary data associated with this article can be found, in the online version, at doi:10.1016/j.photochem.2006.07.005.

References

[1] S. Fukuzumi, K. Yasui, T. Suenobu, K. Ohkubo, M. Fujitsuka, O. Ito, J. Phys. Chem. A 105 (2001) 10501–10510.
[2] B. Konig, H.C. Gallmeier, R. Reichenbach-Klinke, Chem. Commun. (2001) 2390–2391.
[3] S.C. Ritter, M. Eiblmaier, V. Michlova, B. Konig, Tetrahedron 61 (2005) 5241–5251.
[4] C.B. Martin, X.F. Shi, M.L. Tsao, D. Karweik, J. Brooke, C.M. Hadad, M.S. Platz, J. Phys. Chem. B 106 (2002) 10263–10271.
[5] C.B. Martin, M.L. Tsao, C.M. Hadad, M.S. Platz, J. Am. Chem. Soc. 124 (2002) 7226–7234.
[6] R.A. Larson, P.L. Stackhouse, T.L. Crowley, Environ. Sci. Technol. 26 (1992) 1792–1798.
[7] I. Ahmad, Q. Fasihullah, F.H.M. Vaid, J. Photochem. Photobiol. B 78 (2005) 229–234.
[8] W. Holzer, J. Shirdel, P. Zirak, A. Penzkofer, P. Hegemann, R. Deutzmann, E. Hochmuth, Chem. Phys. 308 (2005) 69–78.
[9] I. Ahmad, Q. Fasiliullah, F.H.M. Vaid, J. Photochem. Photobiol. B 75 (2004) 13–20.
[10] C. Banekovich, B. Matuszczak, Tetrahedron Lett. 46 (2005) 5053–5056.
[11] H.J. Grande, C.G. van Schagen, T. Jarbandhan, F. Muller, Helv. Chim. Acta 60 (1977) 348–366.
[12] H.J. Grande, R. Gast, C.G. van Schagen, W.J.H. van Berkel, F. Muller, Helv. Chim. Acta 60 (1977) 367–379.
[13] M.D. Ediger, R.S. Moog, S.G. Boxer, M.P. Fayer, Chem. Phys. Lett. 88 (1982) 123–127.
[14] J. Karolczak, D. Komar, J. Kubicki, T. Wrozowa, K. Dobek, B. Ciesielska, A. Maciejewski, Chem. Phys. Lett. 344 (2001) 154–164.
[15] R. Schmidt, C. Tanielian, R. Dunsbach, C. Wolff, J. Photochem. Photobiol. A 79 (1994) 11–17.
[16] A.R. Horrocks, T. Medinger, F. Wilkinson, Chem. Commun. (1965) 452.
[17] T. Medinger, F. Wilkinson, Trans. Faraday Soc. 61 (1965) 620–630.
[18] A.M. Botelho do Rego, L.F.V. Ferreira, Photonic and electronic spectroscopies for the characterization of organic surfaces and organic molecules adsorbed on surfaces, in: H.S. Nalwa (Ed.), Handbook of Surfaces and Interfaces of Materials, Academic Press, New York, 2001, p. 275.
[19] L.F.V. Ferreira, I.F. Machado, A.S. Oliveira, M.R.V. Ferreira, J.P. Da Silva, J.C. Moreira, J. Phys. Chem. B 106 (2002) 12584–12593.
[20] L.F.V. Ferreira, I.F. Machado, J.P. Da Silva, A.S. Oliveira, Photochem. Photobiol. Sci. 3 (2004) 174–181.
[21] J. Mielcarek, W. Augustyniak, P. Grobelny, G. Nowacka, Int. J. Pharm. 304 (2005) 145–151.
[22] E. Gross, J. Dobson, M. Petersilka, Top. Curr. Chem. 181 (1996) 81–172.
[23] A.D. Becke, J. Chem. Phys. 98 (1993) 5648–5652.
[24] R. Ditchfield, W.J. Hehre, J.A. Pople, J. Chem. Phys. 54 (1971) 724–728.
[25] M.J. Frisch, G.W. Trucks, H.B. Schlegel, G.E. Scuseria, M.A. Robb, J.R. Cheeseman, A.J. Montgomery Jr., T. Vreven, K.N. Kudin, J.C. Burant, J.M. Millam, S.S. Iyengar, J. Tomasi, V. Barone, B. Mennucci, M. Cossi, G. Scalmani, N. Rega, G.A. Petersson, H. Nakatsuji, M. Hada, M. Ehara, K. Toyota, R. Fukuda, J. Hasegawa, M. Ishida, T. Nakajima, Y. Honda, O. Kitao, H. Nakai, M. Klene, X. Li, J.E. Knox, H.P. Hratchian, J.B. Cross, V. Bakken, C. Adamo, J. Jaramillo, R. Gomperts, R.E. Stratmann, O. Yazyev, A.J. Austin, R. Cammi, C. Pomelli, J.W. Ochterski, P.Y. Ayala, K. Morokuma, G.A. Voth, P. Salvador, J.J. Dannenberg, V.G. Zakrzewski, S. Dapprich, A.D. Daniels, M.C. Strain, O. Farkas, D.K. Malick, A.D. Rabuck, K. Raghavachari, J.B. Foresman, J.V. Ortiz, Q. Cui, A.G. Baboul, S. Clifford, J. Cioslowski, B.B. Stefanov, G. Liu, A. Liashenko, P. Piskorz, I. Komaromi, R.L. Martin, D.J. Fox, T. Keith, M.A. Al-Laham, C.Y. Peng, A. Nanayakkara, M. Challacombe, P.M.W. Gill, B. Johnson, W. Chen, M.W. Wong, C. Gonzalez, J.A. Pople, Gaussian 03, revision B.05, Gaussian, Inc., Wallingford CT, 2003.
[26] G.M. Sheldrick, Acta Crystallogr. A 46 (1990) 467–473.
[27] G.M. Sheldrick, SHELXL-97, Program for the Refinement of Crystal Structure, University of Gottingen, Germany, 1997.
[28] M. Ebitani, Y. In, T. Ishida, K.-I. Sakaguchi, J.L. Flippen-Anderson, I.L. Karle, Acta Crystallogr. B B49 (1993) 136–144.
[29] E. Sikorska, I.V. Khmelinskii, A. Komasa, J. Koput, L.F.V. Ferreira, J.R. Herance, J.L. Bourdelande, S.L. Williams, D.R. Worrall, M. Insinska-Rak, M. Sikorski, Chem. Phys. 314 (2005) 239–247.
[30] E.C. Lim, J. Phys. Chem. 90 (1986) 6770–6777.
[31] T.I. Lai, B.T. Lim, E.C. Lim, J. Am. Chem. Soc. 104 (1982) 7631–7635.
[32] F. Wilkinson, W.P. Helman, A.B. Ross, J. Phys. Chem. Ref. Data 22 (1993) 113–262.
[33] R.W. Redmond, J.N. Gamlin, Photochem. Photobiol. 70 (1999) 391–475.
[34] F. Wilkinson, A.A. Abdel-Shafi, J. Phys. Chem. 103 (1999) 5425–5435.
[35] M. Insinska-Rak, E. Sikorska, J.R. Herance, J.L. Bourdelande, I.V. Khmelinskii, M. Kubicki, W. Prukala, I.F. Machado, A. Komasa, L.F.V. Ferreira, M. Sikorski, Photochem. Photobiol. Sci. 4 (2005) 463–468.
[36] M. Insinska-Rak, E. Sikorska, J.L. Bourdelande, I.V. Khmelinskii, W. Prukala, K. Dobek, J. Karolczak, I.F. Machado, L.F.V. Ferreira, A. Komasa, D.R. Worrall, M. Sikorski, J. Mol. Struct. 783 (2006) 184–190.

[37] E. Sikorska, I.V. Khmelinskii, M. Kubicki, W. Prukala, G. Nowacka, A. Siemiarczuk, J. Koput, L.F.V. Ferreira, M. Sikorski, J. Phys. Chem. A 109 (2005) 1785–1794.
[38] Y.L. Pan, R.G. Pinnick, S.C. Hill, S. Niles, S. Holler, J.R. Bottiger, J.P. Wolf, R.K. Chang, Appl. Phys. B-Lasers Optics 72 (2001) 449–454.
[39] P. Drossler, W. Holzer, A. Penzkofer, P. Hegemann, Chem. Phys. 286 (2003) 409–420.
[40] G. Porcal, S.G. Bertolotti, C.M. Previtali, M.V. Encinas, Phys. Chem. Chem. Phys. 5 (2003) 4123–4128.
[41] E. Sikorska, I.V. Khmelinskii, W. Prukala, S.L. Williams, M. Patel, D.R. Worrall, J.L. Bourdelande, J. Koput, M. Sikorski, J. Phys. Chem. A 108 (2004) 1501–1508.